

Yukawa System in One-Dimensional External Field

Hiroo TOTSUJI*, Tokunari KISHIMOTO*, and Chieko TOTSUJI*

(Received January 31 , 1996)

The behavior of the Yukawa system in external one-dimensional force fields is analyzed by the molecular dynamics simulation. The formation of layered structures at low temperatures is observed and the relation between the number of layers and characteristic parameters of the system is obtained. Since the Yukawa system serves as a model of clouds of dust particles in plasmas (dusty plasma) which play an important role in plasma processes of semiconductor engineering, the results may be useful to control the quality of semiconductor wafers in such processes. In simulations, periodic boundary conditions are imposed in two dimensions and deformations of periodic boundaries are allowed in order to reduce the effect of boundaries without giving too much constraint on the symmetry.

1 Introduction

In some processes of semiconductor engineering, plasmas play an important role as an environment which excites reactant gas particles through radio-frequency or microwave radiation. An typical example is the reactive ion etching (RIE).[1] In these plasmas, there usually exist macroscopic particles (dust particles or particulates). Due to difference in the thermal velocities of electrons and ions in plasmas, macroscopic particles have negative charges and negative floating potential. Since the quality of semiconductor wafers obtained by plasma processes depends on the status of plasmas, the control of dust particles in plasma processes is an important problem in semiconductor engineering.

Dust particles in plasmas have negative charges of $-(10^3 \sim 10^4)e$, e being the elementary charge, and their number density is of the order of 10^5cm^{-3} , much smaller than those of plasma particles of the order of 10^9cm^{-3} . With macroscopic size and low densities, macroscopic particles form a system whose structure can be observed by optical methods including naked eyes. Due to screening by surrounding plasma, these macroscopic particles interact with one another via the Yukawa potential. Recently it has been reported that the lattice or ordered structure can be observed under appropriate conditions.[2]

*Department of Electrical and Electronic Engineering

The static and dynamic properties of uniform Yukawa system have long been the subject of study as a simple system which interpolates the systems with short- and long-ranged interactions and also as a model of colloidal suspensions.[3] The phase diagram of uniform system is composed of the fluid and the fcc and bcc solid phases. In recent experiment, however, the structure resembling the hcp solid has been observed.[4, 5, 6, 7] We naturally expect that in experiments the systems are under external force fields and the hcp structure may appear in such nonuniform systems. The purpose of this paper is to analyze the properties of Yukawa system in external fields.

2 Model

2.1 Interaction and External Potentials

Our interest is in the system of macroscopic particles where the degrees of freedom related to plasma particles are averaged out. As a model of systems of macroscopic particles, we take a system composed of particles of one species interacting via the Yukawa interaction

$$v(r) = \frac{q^2}{r} \exp(-r/\lambda). \quad (1)$$

Here q is the charge on a particle, r is the distance, and λ is the screening length.

Macroscopic particles in plasmas are surrounded the sheath whose structure determines the potential around them. As the first approximation of the sheath potential, we may adopt the linearized Debye-Hückel potential which is equivalent to the Yukawa potential. The interaction between colloid particles is given by the DLVO potential. In the limit where the mean distance is much larger than the particle radius, the DLVO potential reduces to the Yukawa potential. We may thus regard macroscopic particles in plasmas and colloidal suspensions as Yukawa system.

In order to simulate such a systems in external fields, we apply the one-dimensional potential in the direction of z axis

$$v_{ext}(z) = \frac{k}{2} z^2. \quad (2)$$

We thus have a system confined near $z = 0$ and k is a constant characterizing the strength of confinement.

In real systems, the gravitational force is balanced by the static electric field or other force fields. Near the equilibrium point, the total potential may be expressed by a quadratic function without linear term. The above form of our potential may simulate these potentials near the equilibrium point. We also assume that the potential is one-dimensional for simplicity. This also corresponds to real experiments at least in the central part of the system.

2.2 Characteristic Parameters and Phase Diagram of Uniform System

Let us denote the number density of macroscopic particles by n and define the mean distance a by

$$n = \frac{3}{4\pi a^3}. \quad (3)$$

Our system in thermal equilibrium at the temperature T is characterized by two independent dimensionless parameters. In this paper we take these parameters to be

$$\Gamma = \frac{q^2}{ak_B T}, \quad (4)$$

and

$$\xi = \frac{a}{\lambda}. \quad (5)$$

In the limit of long screening length, or $\xi \rightarrow 0$, our system reduces to the one-component plasma (OCP). In OCP, we have a phase transition between the fluid and the bcc solid at $\Gamma \sim 178$. [8]

When the parameter ξ is large, we have a system of particles interacting through a short-ranged potential. In this case, we expect the fluid and the fcc solid phases.

The phase diagram of the uniform Yukawa system is shown in Fig.1. [9] We have the bcc solid when ξ is small and the fcc solid when ξ is large. This is consistent with our expectation based on the behaviors in limiting cases. Since the effect of screening may be estimated at the mean distance a , the relation $\Gamma \exp(-\xi) = 178$ may approximately give the boundary of fluid and solid phases. This relation is also plotted in Fig.1 and we see it works as a first approximation.

When the one-dimensional external field (2) is imposed on the Yukawa system, our particles are confined near the plane $z = 0$. In this case, the mean distance may be defined by, instead of (3),

$$N_s = \frac{1}{\pi a^2} \quad (6)$$

where N_s is the areal number density in xy -plane. We also have another independent dimensionless parameter related to the strength of confinement. As such, we may take

$$\frac{ka^2}{k_B T}. \quad (7)$$

At low temperatures, the uniform Yukawa system is characterized by the unique parameter ξ . The transition between the fcc and bcc solids occurs around $\xi \sim 2.5$. With one-dimensional external potential, our system is characterized by two parameters. In this paper we use ξ and the ratio

$$\frac{q^2/a}{ka^2} \quad (8)$$

as two independent parameters.

2.3 Numerical Methods

We impose the periodic boundary condition in the x and y directions which are perpendicular to the direction of external field and perform the molecular dynamics simulation. Since the shape of the unit cell in two-dimensions may have strong effects on the distribution of particles, we allow the deformation of fundamental vectors of two-dimensional periodic boundary conditions.

We define the 2×2 tensor \mathbf{h} composed of fundamental (column) vectors of periodicity \mathbf{a} and \mathbf{b} as

$$\mathbf{h} = (\mathbf{a}, \mathbf{b}). \quad (9)$$

and express the coordinate

$$\mathbf{r} = (\mathbf{R}, z) \quad (10)$$

or

$$\mathbf{r} = \mathbf{R} + z\hat{z} \quad (11)$$

as

$$\mathbf{R} = \mathbf{h} \cdot \mathbf{X}. \quad (12)$$

The Lagrangian of our system is given by

$$\mathcal{L}(\{\mathbf{X}_i, z_i, \dot{\mathbf{X}}_i, \dot{z}_i\}, \mathbf{h}, \dot{\mathbf{h}}) = \sum_i \frac{m_i}{2} \dot{\mathbf{X}}_i^t \cdot \mathbf{G} \cdot \dot{\mathbf{X}}_i + \sum_i \frac{m_i}{2} \dot{z}_i \dot{z}_i - U(\mathbf{h}, \{\mathbf{X}_i, z_i\}) + \frac{W}{2} \text{Tr} [\dot{\mathbf{h}}^t \cdot \dot{\mathbf{h}}]. \quad (13)$$

Here U is the interaction energy given in Appendix and

$$\mathbf{G} = \mathbf{h}^t \cdot \mathbf{h}. \quad (14)$$

Velocities in two dimensions are *defined* by

$$\dot{\mathbf{R}}_i \equiv \mathbf{h} \cdot \dot{\mathbf{X}}_i. \quad (15)$$

Equations of motion are given by

$$\frac{d}{dt} \left(\frac{\partial \mathcal{L}}{\partial \dot{\mathbf{X}}_i} \right) - \frac{\partial \mathcal{L}}{\partial \mathbf{X}_i} = 0, \quad (16)$$

$$\frac{d}{dt} \left(\frac{\partial \mathcal{L}}{\partial \dot{z}_i} \right) - \frac{\partial \mathcal{L}}{\partial z_i} = 0, \quad (17)$$

and

$$\frac{d}{dt} \left(\frac{\partial \mathcal{L}}{\partial \dot{h}_{\alpha\beta}} \right) - \frac{\partial \mathcal{L}}{\partial h_{\alpha\beta}} = 0, \quad (18)$$

or

$$m_i \frac{d}{dt} \mathbf{G} \cdot \frac{d}{dt} \mathbf{X}_i = - \frac{\partial}{\partial \mathbf{X}_i} U, \quad (19)$$

$$m_i \frac{d^2}{dt^2} z_i = - \frac{\partial}{\partial z_i} U, \quad (20)$$

and

$$W \frac{d^2}{dt^2} \mathbf{h} = \Pi \cdot \sigma. \quad (21)$$

For Yukawa system with two-dimensional periodicity $\{\mathbf{P}\}$ in the xy plane, Π is defined by

$$\Pi = \frac{1}{V_0} \left\{ \sum_i m_i (\mathbf{h} \cdot \mathbf{X}_i) (\mathbf{h} \cdot \mathbf{X}_i) - \frac{1}{2} \sum_{i \neq j} \sum_{\mathbf{P}} \frac{(\mathbf{R}_{ij} - \mathbf{P})(\mathbf{R}_{ij} - \mathbf{P})}{|\mathbf{r}_{ij} - \mathbf{P}|} \frac{\partial}{\partial |\mathbf{r}_{ij} - \mathbf{P}|} v(|\mathbf{r}_{ij} - \mathbf{P}|) \right\} + \Pi_0 \quad (22)$$

and

$$\Pi_0 = - \frac{N}{2V_0} \sum_{\mathbf{P} \neq 0} \frac{\mathbf{P}\mathbf{P}}{P} \frac{\partial}{\partial P} v(P), \quad (23)$$

$$\sigma = V_0 (\mathbf{h}^t)^{-1}. \quad (24)$$

Here V_0 is the volume (area) of the unit cell in two dimensions. Detailed expressions of terms in Π are given in Appendix.

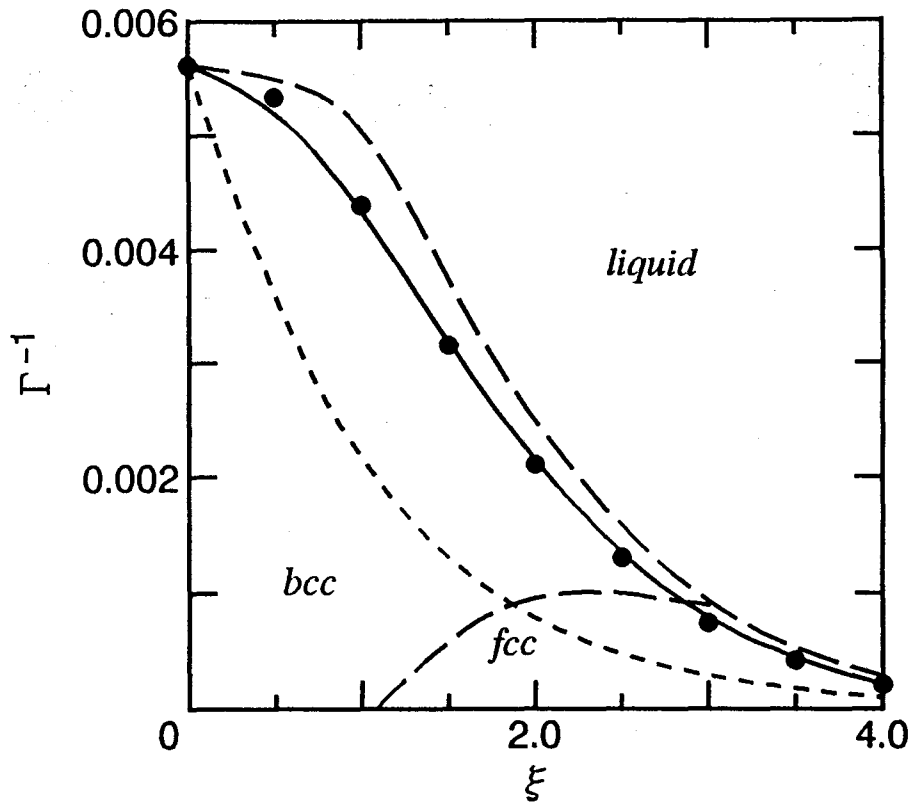


Figure 1: Phase diagram of Yukawa system. Solid line is the boundary of fluid and solid phases. Broken line is due to Robbins *et al.* and dotted line expresses the relation $\Gamma \exp(-\xi) = 178$.

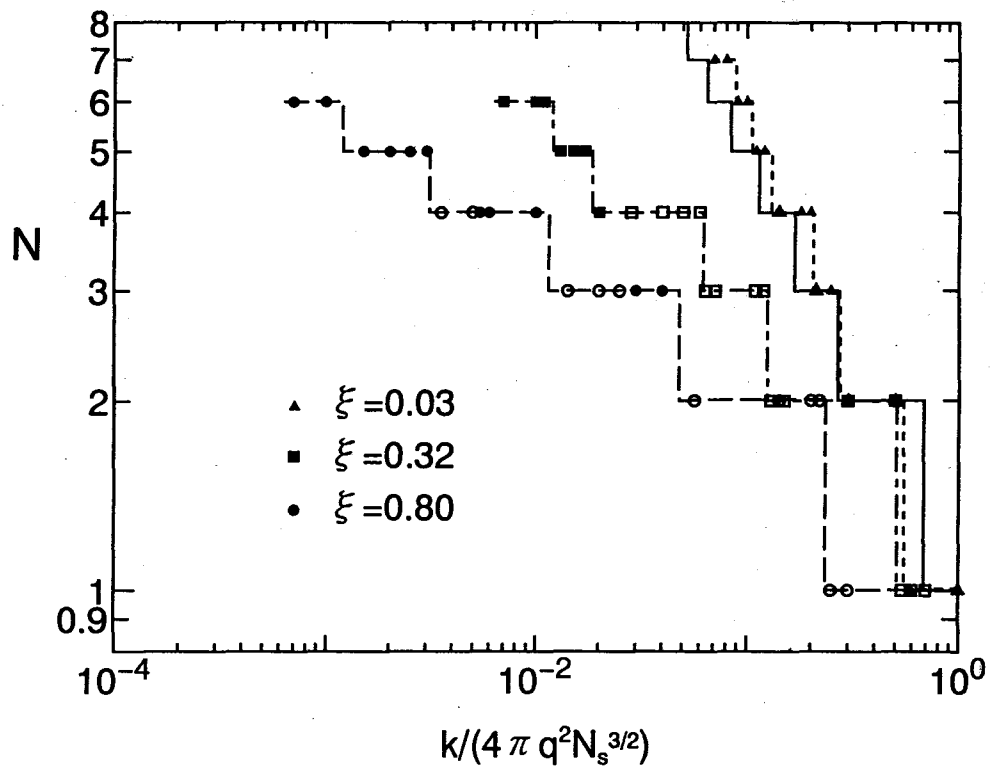


Figure 3: Number of layers as function of ξ and $k/q^2 N_s^{3/2}$. Solid line is theoretical result for one-component plasma or $\xi = 0$. Open symbols are obtained by simulations with smaller number of particles.

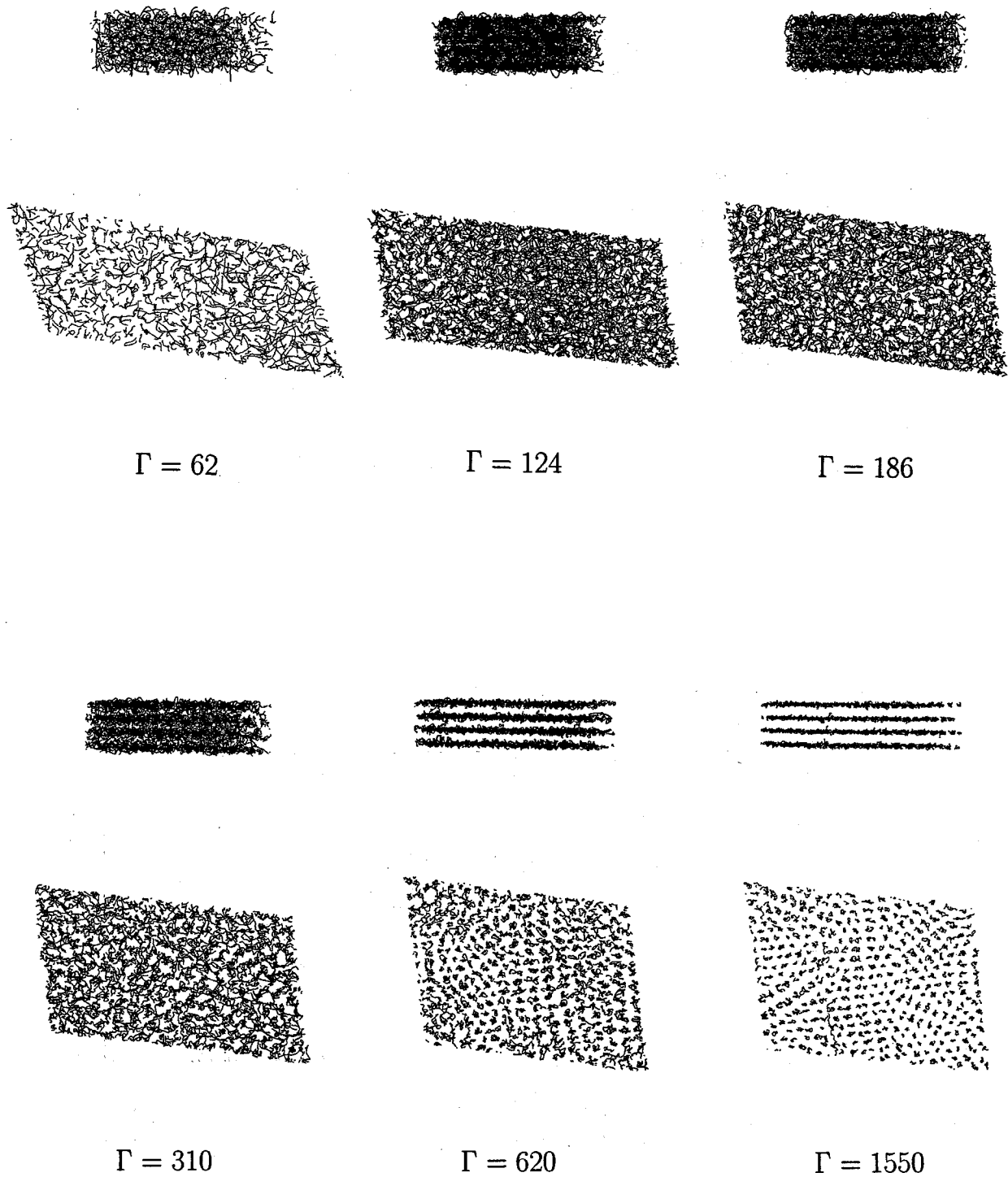
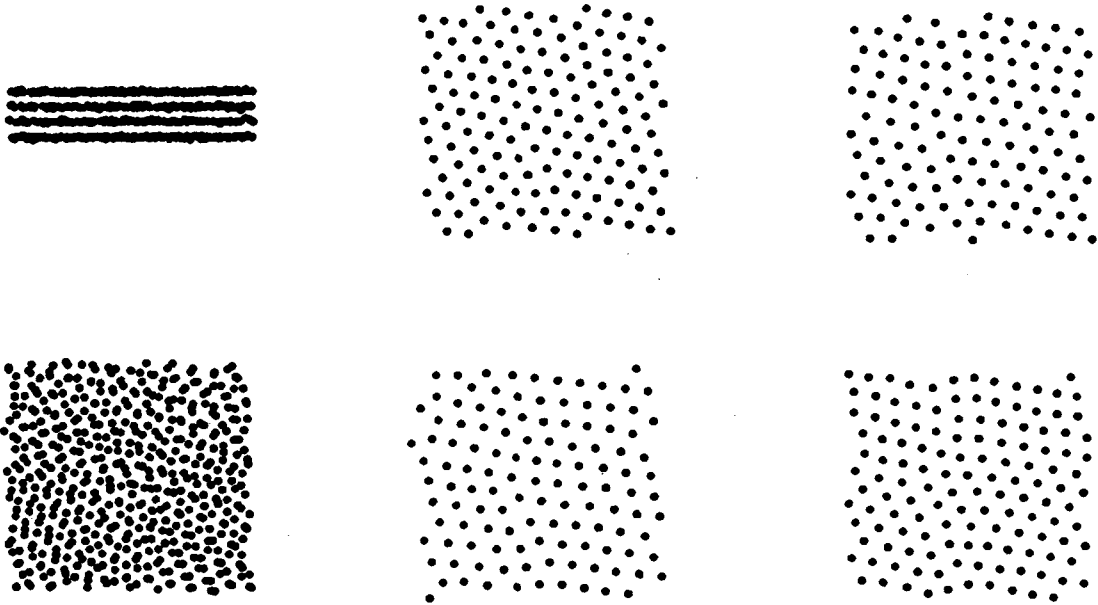


Figure 2: Temperature dependence of particle distribution. Orbits in xz -plane and xy -planes are shown. Values of ξ and $k/4\pi q^2 N_s^{3/2}$ are 0.8 and 0.006, respectively.

$$\xi = 0.03 \quad \frac{k}{4\pi q^2 N_s^{3/2}} = 0.2$$



$$\xi = 0.8 \quad \frac{k}{4\pi q^2 N_s^{3/2}} = 0.01$$



Figure 4: Two examples of two-dimensional distributions in layers. In each group of data, columns at center and right are orbits in each layer. Left column is orbits of all particles in xz -plane (upper) and xy -plane (lower).

3 Formation of Layers

Our particles are confined around the plane $z = 0$ by the external potential. When the temperature is high, particles form a cloud parallel to the plane $z = 0$ and we have no microscopic structure. At sufficiently low temperatures, we observe the appearance of layers parallel to the xy -plane. The behavior of the cloud at different temperatures is shown in Fig.2.

The number of layers at low temperatures is related to the parameter of our system. At sufficiently low temperatures, our system is characterized by two dimensionless parameters given by ξ and (8).

When the confining force is sufficiently strong, particles are forced to be in the plane $z = 0$: Particles are interacting through the repulsive force but the effect of confining force overwhelms the mutual repulsion. With the decrease of the confining force, the effect of mutual repulsion manifests itself and the thickness of particle distribution increases. The relation between the number of layers and the characteristic parameters of our system is shown in Fig.3. These results are mainly obtained by simulations with 512 independent particles.

In the case of one-component plasma, it has been shown both experimentally and theoretically that confined finite system forms layers in accordance with the geometry of confinement.[10] In the limit of small screening constant, our system reduces to the one-component plasma. As is shown in Fig.3, our results are consistent with this limiting behavior.

With the increase of the screening constant, the repulsive interaction between particles becomes weak and the number of layers is expected to decrease. We observe this tendency in Fig.3. When $\xi \rightarrow 0$, however, our results seem to be slightly inconsistent with those for OCP ($\xi = 0$). This may be due to approximate nature of the latter which is derived theoretically.

Some examples of the distribution of particles in each layer is shown in Fig.4. There appear structures of both the three-fold and four-fold symmetries. In the case of colloidal suspensions confined between glass plates, systematic changes of the symmetry with the increase or decrease of the number of layers have been observed.[11] Our result, however, is not sufficient to make definite statement on the relation between the symmetry and the number of layers.

4 Conclusion

Numerical simulations of the Yukawa system in external force fields have been performed as a model of dusty plasmas in plasma processes of semiconductor engineering. It has been shown that the Yukawa system confined by one-dimensional external potential forms layers which are perpendicular to the direction of the external force at low temperatures. The number of layers is determined as a function of system parameters. The results may be useful to determine the system parameters such as the density of particle or the external force parameters and control the behavior of dusty plasmas which is closely related to the quality of semiconductor wafers obtained by plasma processes.

Acknowledgments

The authors would like to thank Mr. Y. Inoue and Professor S. Nara for numerical work and discussions in related researches on the Yukawa system. This work has been partly supported by the Grant-in-Aid for Scientific Research from the Ministry of Education, Science, Sports, and Culture No.06680448.

Appendix

The interaction energy U is given by

$$\begin{aligned}
\frac{U}{e^2} &= \frac{1}{2} \sum_{i \neq j}^N \sum_{\mathbf{P}} \frac{1}{|\mathbf{r}_{ij} - \mathbf{P}|} \exp(-\kappa|\mathbf{r}_{ij} - \mathbf{P}|) + \frac{N}{2} \phi_0 \\
&= \frac{1}{2} \sum_{i \neq j}^N \sum_{\mathbf{P}} \frac{1}{2|\mathbf{P} - \mathbf{r}_{ij}|} \left\{ \exp(\kappa|\mathbf{P} - \mathbf{r}_{ij}|) \operatorname{erfc} \left(G|\mathbf{P} - \mathbf{r}_{ij}| + \frac{\kappa}{2G} \right) \right. \\
&\quad \left. + \exp(-\kappa|\mathbf{P} - \mathbf{r}_{ij}|) \operatorname{erfc} \left(G|\mathbf{P} - \mathbf{r}_{ij}| - \frac{\kappa}{2G} \right) \right\} \\
&\quad + \frac{1}{2S_0} \sum_{i,j} \sum_{\mathbf{K}} \frac{\pi}{\sqrt{K^2 + \kappa^2}} \exp(i\mathbf{K} \cdot \mathbf{R}_{ij}) \\
&\quad \times \left(\exp(\sqrt{K^2 + \kappa^2}|z_{ij}|) \operatorname{erfc} \left(\frac{\sqrt{K^2 + \kappa^2}}{2G} + G|z_{ij}| \right) \right. \\
&\quad \left. + \exp(-\sqrt{K^2 + \kappa^2}|z_{ij}|) \operatorname{erfc} \left(\frac{\sqrt{K^2 + \kappa^2}}{2G} - G|z_{ij}| \right) \right) \\
&\quad + \frac{N}{2} \sum_{\mathbf{P}}' \frac{1}{2P} \left\{ \exp(\kappa P) \operatorname{erfc} \left(GP + \frac{\kappa}{2G} \right) + \exp(-\kappa P) \operatorname{erfc} \left(GP - \frac{\kappa}{2G} \right) \right\} \\
&\quad + \frac{N}{2} \left[\kappa \operatorname{erfc} \left(\frac{\kappa}{2G} \right) - \frac{2}{\sqrt{\pi}} G \exp \left(-\frac{\kappa^2}{4G^2} \right) \right]. \tag{25}
\end{aligned}$$

The force is given by the derivatives of U as

$$\frac{\partial}{\partial \mathbf{X}_i} U = \mathbf{h}^i \cdot \frac{\partial}{\partial \mathbf{R}_i} U, \tag{26}$$

$$\begin{aligned}
-\frac{\partial U}{\partial \mathbf{R}_i e^2} &= \sum_{j(\neq i)} \sum_{\mathbf{P}} \frac{(\mathbf{r}_i - \mathbf{r}_j - \mathbf{P})}{|\mathbf{r}_{ij} - \mathbf{P}|^3} \\
&\quad \times \left[\frac{1}{2} (1 - \kappa|\mathbf{r}_{ij} - \mathbf{P}|) \exp(\kappa|\mathbf{r}_{ij} - \mathbf{P}|) \operatorname{erfc} \left(G|\mathbf{r}_{ij} - \mathbf{P}| + \frac{\kappa}{2G} \right) \right. \\
&\quad \left. + \frac{1}{2} (1 + \kappa|\mathbf{r}_{ij} - \mathbf{P}|) \exp(-\kappa|\mathbf{r}_{ij} - \mathbf{P}|) \operatorname{erfc} \left(G|\mathbf{r}_{ij} - \mathbf{P}| - \frac{\kappa}{2G} \right) \right. \\
&\quad \left. + \frac{2}{\sqrt{\pi}} G|\mathbf{r}_{ij} - \mathbf{P}| \exp \left(-G^2|\mathbf{r}_{ij} - \mathbf{P}|^2 - \frac{\kappa^2}{4G^2} \right) \right] \\
&\quad - \frac{1}{S_0} \sum_{\mathbf{K}} \frac{\pi}{\sqrt{K^2 + \kappa^2}} i\mathbf{K} \sum_j^N \exp(i\mathbf{K} \cdot \mathbf{R}_{ij}) \\
&\quad \times \left(\exp(\sqrt{K^2 + \kappa^2}|z_{ij}|) \operatorname{erfc} \left(\frac{\sqrt{K^2 + \kappa^2}}{2G} + G|z_{ij}| \right) \right.
\end{aligned}$$

$$+ \exp(-\sqrt{K^2 + \kappa^2}|z_{ij}|) \operatorname{erfc}\left(\frac{\sqrt{K^2 + \kappa^2}}{2G} - G|z_{ij}|\right), \quad (27)$$

and

$$\begin{aligned} -\frac{\partial U}{\partial z_i e^2} &= \sum_{j(\neq i)} \sum_{\mathbf{P}} \frac{z_{ij}}{|\mathbf{r}_{ij} - \mathbf{P}|^3} \\ &\times \left[\frac{1}{2} (1 - \kappa|\mathbf{r}_{ij} - \mathbf{P}|) \exp(\kappa|\mathbf{r}_{ij} - \mathbf{P}|) \operatorname{erfc}\left(G|\mathbf{r}_{ij} - \mathbf{P}| + \frac{\kappa}{2G}\right) \right. \\ &+ \frac{1}{2} (1 + \kappa|\mathbf{r}_{ij} - \mathbf{P}|) \exp(-\kappa|\mathbf{r}_{ij} - \mathbf{P}|) \operatorname{erfc}\left(G|\mathbf{r}_{ij} - \mathbf{P}| - \frac{\kappa}{2G}\right) \\ &+ \frac{2}{\sqrt{\pi}} G|\mathbf{r}_{ij} - \mathbf{P}| \exp\left(-G^2|\mathbf{r}_{ij} - \mathbf{P}|^2 - \frac{\kappa^2}{4G^2}\right) \left. \right] \\ &- \frac{1}{S_0} \sum_{\mathbf{K}} \pi \sum_j^N \operatorname{sign}(z_{ij}) \exp(i\mathbf{K} \cdot \mathbf{R}_{ij}) \\ &\times \left(\exp(\sqrt{K^2 + \kappa^2}|z_{ij}|) \operatorname{erfc}\left(\frac{\sqrt{K^2 + \kappa^2}}{2G} + G|z_{ij}|\right) \right. \\ &\left. - \exp(-\sqrt{K^2 + \kappa^2}|z_{ij}|) \operatorname{erfc}\left(\frac{\sqrt{K^2 + \kappa^2}}{2G} - G|z_{ij}|\right) \right). \quad (28) \end{aligned}$$

The pressure tensor is given by

$$\begin{aligned} \frac{V_0}{q^2} \Pi &= \frac{1}{q^2} \sum_{i=1}^N m_i (\mathbf{h} \cdot \dot{\mathbf{X}}_i) (\mathbf{h} \cdot \dot{\mathbf{X}}_i) \\ &+ \frac{1}{2} \sum_{i \neq j} \sum_{\mathbf{P}} \frac{(\mathbf{r}_{ij} - \mathbf{P})(\mathbf{r}_{ij} - \mathbf{P})}{|\mathbf{r}_{ij} - \mathbf{P}|^3} \left\{ \frac{1}{2} (1 - \kappa|\mathbf{r}_{ij} - \mathbf{P}|) \exp(\kappa|\mathbf{r}_{ij} - \mathbf{P}|) \operatorname{erfc}\left(G|\mathbf{r}_{ij} - \mathbf{P}| + \frac{\kappa}{2G}\right) \right. \\ &+ \frac{1}{2} (1 + \kappa|\mathbf{r}_{ij} - \mathbf{P}|) \exp(-\kappa|\mathbf{r}_{ij} - \mathbf{P}|) \operatorname{erfc}\left(G|\mathbf{r}_{ij} - \mathbf{P}| - \frac{\kappa}{2G}\right) \\ &+ \frac{2}{\sqrt{\pi}} G|\mathbf{r}_{ij} - \mathbf{P}| \exp\left(-G^2|\mathbf{r}_{ij} - \mathbf{P}|^2 - \frac{\kappa^2}{4G^2}\right) \left. \right\} \\ &- \frac{1}{2S_0} \sum_{i \neq j} \sum_{\mathbf{K}} \frac{1}{2\pi} \int_{-\infty}^{\infty} dg_z \mathbf{K} \mathbf{K} \frac{8\pi}{(g^2 + \kappa^2)^2} \left(\frac{g^2 + \kappa^2}{4G^2} + 1 \right) \exp\left(-\frac{g^2 + \kappa^2}{4G^2} + i\mathbf{g} \cdot \mathbf{r}_{ij}\right) \\ &+ \frac{1}{2S_0} \sum_{i \neq j} \sum_{\mathbf{K}} \frac{1}{2\pi} \int_{-\infty}^{\infty} dg_z \frac{4\pi}{g^2 + \kappa^2} \exp\left(-\frac{g^2 + \kappa^2}{4G^2} + i\mathbf{g} \cdot \mathbf{r}_{ij}\right) \\ &+ \frac{N}{2} \sum_{\mathbf{P} \neq 0} \frac{\mathbf{P} \mathbf{P}}{P^3} \left\{ \frac{1}{2} (1 - \kappa P) \exp(\kappa P) \operatorname{erfc}\left(GP + \frac{\kappa}{2G}\right) \right. \\ &+ \frac{1}{2} (1 + \kappa P) \exp(-\kappa P) \operatorname{erfc}\left(GP - \frac{\kappa}{2G}\right) \\ &+ \frac{2}{\sqrt{\pi}} GP \exp\left(-G^2 P^2 - \frac{\kappa^2}{4G^2}\right) \left. \right\} \\ &- \frac{N}{2S_0} \sum_{\mathbf{K}} \frac{1}{2\pi} \int_{-\infty}^{\infty} dg_z \mathbf{K} \mathbf{K} \frac{8\pi}{(g^2 + \kappa^2)^2} \left(\frac{g^2 + \kappa^2}{4G^2} + 1 \right) \exp\left(-\frac{g^2 + \kappa^2}{4G^2}\right) \\ &+ \frac{N}{2S_0} \sum_{\mathbf{K}} \frac{1}{2\pi} \int_{-\infty}^{\infty} dg_z \frac{4\pi}{g^2 + \kappa^2} \exp\left(-\frac{g^2 + \kappa^2}{4G^2}\right). \quad (29) \end{aligned}$$

References

- [1] For example, *VLSI Technology*, second ed. (ed. S. M. Sze, McGraw-Hill, 1988), Chap.5.
- [2] H. Ikezi, *Phys. Fluids* **29**, 1764(1986).
- [3] For example, M. O. Robbins, K. Kremer, and G. S. Grest, *J. Chem. Phys.* **88**, 3286(1988).
- [4] H. Thomas, G. E. Morfill, V. Demmel, J. Goree, B. Feuerbacher, and D. Möhlmann, *Phys. Rev. Lett.* **73**, 652(1994).
- [5] J. H. Chu and Lin I, *Physica A* **205**, 183(1994): *Phys. Rev. Lett.* **72**, 4009(1994).
- [6] Y. Hayashi and T. Tachibana, *Jpn. J. Appl. Phys.* **33**, L804(1994).
- [7] A. Melzer, T. Trottenberg, and A. Piel, *Phys. Lett. A* **191**, 301(1994).
- [8] W. L. Slattery, G. D. Doolen, and H. E. Dewitt, *Phys. Rev. A* **26**, 2255(1982).
- [9] Y. Inoue, Master Thesis, Department of Electrical and Electronic Engineering, Okayama University, March 1995.
- [10] H. Totsuji, *Strongly Coupled Plasma Physics* (ed. S. Ichimaru, Elsevier Science Publishers, 1990), p. 213.
- [11] D. H. Van Winkle and C. A. Murray, *Phys. Rev. A* **34**, 562(1986).